New Journal of Physics
The open access journal at the forefront of physics

Deutsche Physikalische Gesellschaft DPG
IOP Institute of Physics

Published in partnership with: Deutsche Physikalische Gesellschaft and the Institute of Physics

OPEN ACCESS

RECEIVED
16 July 2021

REVISED
20 September 2021

ACCEPTED FOR PUBLICATION
27 October 2021

PUBLISHED
18 November 2021

PAPER

Acoustic geometric-phase meta-array

Bingyi Liu[1], Zhaoxian Su[1], Yong Zeng[2], Yongtian Wang[1], Lingling Huang[1,*] and Shuang Zhang[3,4,*]

[1] School of Optics and Photonics, Beijing Engineering Research Center of Mixed Reality and Advanced Display, Beijing Institute of Technology, Beijing, 100081, People's Republic of China
[2] Faculty of Materials and Manufacturing, Beijing University of Technology, Beijing, 100124, People's Republic of China
[3] Department of Physics, The University of Hong Kong, Hong Kong, People's Republic of China
[4] Department of Electrical and Electronic Engineering, The University of Hong Kong, Hong Kong, People's Republic of China
[*] Authors to whom any correspondence should be addressed.

E-mail: huanglingling@bit.edu.cn and shuzhang@hku.hk

Keywords: acoustic, vortex beam, geometric phase, topological charge, metalens

Supplementary material for this article is available online

Abstract

Metasurfaces based on geometric phase acquired from the conversion of the optical spin states provide a robust control over the wavefront of light, and have been widely employed for construction of various types of functional metasurface devices. However, this powerful approach cannot be readily transferred to the manipulation of acoustic waves because acoustic waves do not possess the spin degree of freedom. Here, we propose the concept of acoustic geometric-phase meta-array by leveraging the conversion of orbital angular momentum of acoustic waves, where well-defined geometric-phases can be attained through versatile topological charge conversion processes. This work extends the concept of geometric-phase metasurface from optics to acoustics, and provides a new route for acoustic wave control.

1. Introduction

Geometric-phase metasurfaces (GPMs) have been widely employed as an efficient and robust means to control the scattering of electromagnetic waves with the controllable geometric phase acquired via a spin conversion process [1–3]. Due to the simple relationship between the geometric phase and the orientation of anisotropic nanostructures for generating the spin conversion, GPMs can be used for flexible wavefront manipulation, such as imaging [4, 5], holography [6, 7], harmonic generations [8, 9], trapping [10, 11], quantum technology [12, 13], etc. However, this concept cannot be directly extended to acoustics due to the lack of such spin conversion process in acoustics, even though the concept of acoustic spin has been recently proposed [14, 15]. Therefore, the common strategies involved in the design of acoustic metasurfaces or metamaterials mainly focus on acoustic surface impedance engineering and effective acoustic refractive index modulation, such as Helmholtz resonators [16–20], grooves [21–24], coiling-space structures [25–29], pentamode metamaterials [30], mass-membrane system [31], just to name a few. Generally, the functionality of acoustic meta-atoms (e.g. designated phase shift) is fixed once the geometry of the structures is determined. Hence, acoustic metasurfaces usually require precise spatial arrangement of the meta-atoms by following a rigorous meta-device design procedure [32]. As a result, recent works on tunable acoustic meta-atoms suffer from the resonance-based phase delay, which unavoidably couples with the transmission amplitude and requires delicate control over some critical geometry parameters [33–35].

In this work, we propose a reconfigurable acoustic meta-array based on acoustic geometric phases which are obtained through versatile acoustic vortex topological charge (TC) conversion occurring within each pixel of the meta-array—a cylindrical acoustic waveguide with judiciously engineered interior structures. Each meta-pixel waveguide, containing a number of acoustic geometric meta-plates (AGM), is designed to implement sequential manipulations on the incident acoustic wave including generation and conversion of

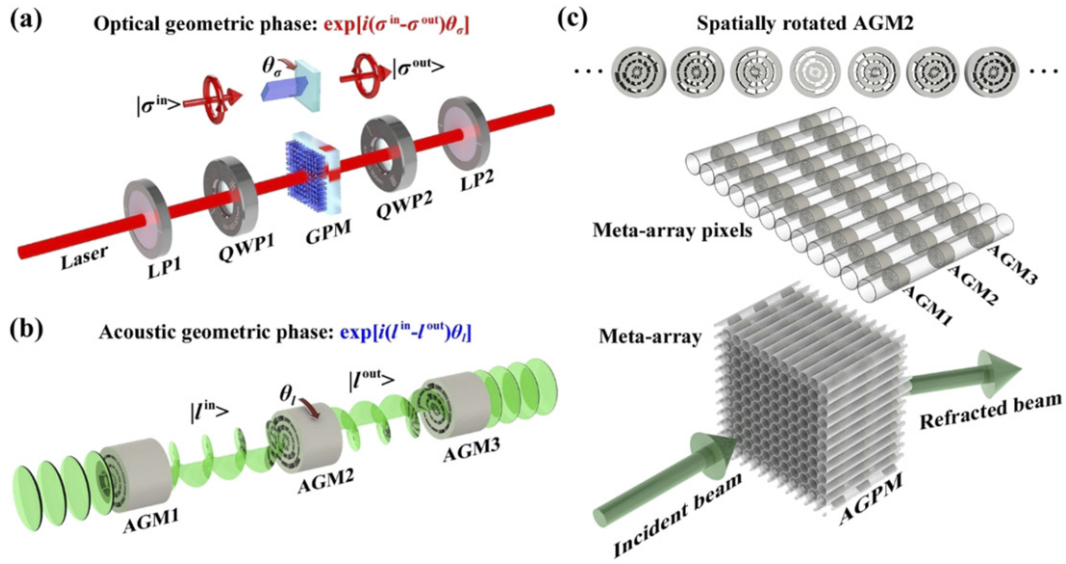

Figure 1. Analogy between the (a) optical and (b) acoustic geometric phase obtained through scattering processes in meta-atoms. LP, QWP and GPM refer to the linear polarizer, quarter wave plate and optical GPM, respectively. AGMs refer to the acoustic meta-plates designed for TC generation, conversion and detection. (c) The anomalous beam bending (green arrows) realized with the acoustic geometric-phase meta-array (AGPM). Meta-array pixel consists of the cylindrical waveguides and several AGMs to support the TC conversion processes. The phase gradient is obtained by spatially rotating the TC converted AGMs.

vortex beams of various TCs. A geometric phase arises from the conversion between two different orbital angular momenta, which can be continuously controlled by varying the orientation of the conversion element, i.e. the AGM for the designated TC conversion process, while the transmitted amplitude almost remains unchanged. As a proof of principle, flexible acoustic field manipulations including acoustic beam steering and focusing can be realized with the proposed geometric-phase meta-array. Our design opens a new avenue for flexible acoustic field generation and the controllable phase manipulation.

2. Principle of acoustic geometric phase

We start by a brief description of the geometric phase with optical metasurfaces. When a circularly polarized light is incident onto a GPM, the transmitted light carries a geometric phase term of $\exp\left[i\left(\sigma^{\text{in}}-\sigma^{\text{out}}\right)\theta_\sigma\right]$, where σ^{in} and σ^{out} refer to the spin of input and output circularly polarized light, θ_σ is the orientation angle of the nanoantenna, as illustrated by figure 1(a). Therefore, only the cross-polarized component of the transmitted light, i.e. $\sigma^{\text{out}}=-\sigma^{\text{in}}$, carries the geometric phase term of $\exp\left(2i\sigma^{\text{in}}\theta_\sigma\right)$. Thus, the wavefront of the cross-polarized transmitted beam can be arbitrarily controlled by adjusting the orientation angles of the nanoantennas across the metasurface. Here, we show that this geometric phase also accompanies a conversion process between different orbital angular momenta in a cylindrical waveguide, and therefore the same principle can be applied to acoustics where spin degree of freedom does not exist. Specifically, when an acoustic meta-plate converts the vortex of an incident acoustic beam from TC l^{in} to TC l^{out}, the TC-converted acoustic beam could carry an additional phase modulation of $\exp\left[i\left(l^{\text{in}}-l^{\text{out}}\right)\theta_l\right]$, where θ_l is the orientation angle of the acoustic meta-plate responsible for this conversion, as illustrated by figure 1(b). Figure 1(c) shows the schematic of anomalous beam bending achieved with an acoustic geometric-phase meta-array, where the spatially rotated AGMs inside the meta-array pixels encode the desired phase gradient.

In order to understand the mechanism of the presence of the acoustic geometric phase obtained through TC conversions, we consider a general TC conversion case which involves the orbital angular momentum transfer from TC l^{in} to TC l^{out}. By defining the complex transmission of an AGM of TC l^{ξ} and orientation angle θ_l as $\hat{T}(\theta_l)$, then we have:

$$|l^{\text{out}}\rangle=\hat{T}(\theta_l)\,|l^{\text{in}}\rangle. \tag{1}$$

By rotating the incident beam, the transmission beam, and the AGM in the counter-clockwise direction about the propagation axis by an angle φ, the above equation still holds for the transformed waves. Considering the additional phase acquired by the incident and transmitted beams due to the rotation (see

supplementary material (https://stacks.iop.org/NJP/23/113026/mmedia) [36]), one can write:

$$\exp\left(-il^{\text{out}}\varphi\right)|l^{\text{out}}\rangle = \hat{T}(\theta_l+\varphi)\exp\left(-il^{\text{in}}\varphi\right)|l^{\text{in}}\rangle. \tag{2}$$

By combing equations (1) and (2), it is straightforward to show $\hat{T}(\theta_l+\varphi) = \hat{T}(\theta_l)\exp\left[i\left(l^{\text{in}}-l^{\text{out}}\right)\varphi\right]$, and by selecting θ_l to be zero, we arrive at the following simple expression for the geometric phase as a function of orientation angle φ:

$$\hat{T}(\varphi) = \hat{T}(0)\exp\left[i\left(l^{\text{in}}-l^{\text{out}}\right)\varphi\right]. \tag{3}$$

Hence, the overall geometric phase carried by the transmitted field is $\exp\left[i\left(l^{\text{in}}-l^{\text{out}}\right)\varphi\right]$.

Thus, various types of geometric-phase modulations are available via different TC conversion processes. For example, for an incident beam of TC $l^{\text{in}}=1$, with an acoustic meta-plate of TC $l^{\xi}=1$, the transmitted acoustic wave would have a TC $l^{\text{out}}=0$ and carry the geometric phase of $\exp(i\theta_l)$ when rotating the acoustic meta-plate by angle of θ_l. Moreover, by converting an acoustic vortex beam of TC $l^{\text{in}}=\pm1$ to the vortex of TC $l^{\text{out}}=\mp1$ through an acoustic meta-plate of TC $l^{\xi}=2$, the corresponding geometric-phase modulation of transmitted acoustic wave is $\exp(\pm2i\theta_l)$. Generally, the acoustic geometric phase $\exp\left(qi\theta_l\right)$, $q=\pm1,\pm2,\ldots$ can be obtained at will by selecting appropriate TC conversion process.

3. Design principle of acoustic geometric-phase meta-array

Ideally, an AGM can be constructed by dividing it into many sections along the azimuthal direction and by filling different sections with acoustic material of gradually varying refractive indices but with the same impedance matched to that of air, as shown in figure 2(a). Here, the AGM is placed inside a rigid waveguide of inner radius R, and it contains l^{ξ} repeating units along the azimuthal direction. Each unit consists of M number of sections to achieve a phase variation of 2π at the operating wavelength λ_0. Thus, the refractive index of the mth section within each repeating unit is given as $n_m = 1+(m-1)\lambda_0/Mh$, where h is the thickness of AGM and $m=1,2,\ldots,M$, with the corresponding sector angle of each section being $2\pi/\left(l^{\xi}M\right)$.

The numerical calculation is conducted with the finite element method, details of the simulation setup can be found in supplementary material [36]. Figures 2(b) and (c) show the geometric-phase modulation obtained through the TC conversion processes. Here, the acoustic meta-plate consists of 12 sections, and the operating wavelength is selected as 10 cm. In the first case shown in figure 2(b), the vortex of TC $l=1$ is firstly generated through $|0\rangle\rightarrow|1\rangle$ process via an AGM of TC $l^{\xi}=-1$, and then converted into a plane acoustic wave via $|1\rangle\rightarrow|0\rangle$ process by a second AGM of TC $l^{\xi}=+1$. The orientation of the first AGM is fixed while that of the second one (θ_l) is varied to provide a geometric phase of $\exp(i\theta_l)$ (figure 2(d)). In the second example, the geometric phase obtained through the TC conversion process $|1\rangle\rightarrow|-1\rangle$ is illustrated in figure 2(c). In this configuration, three AGMs are employed, i.e. vortex source generation (AGM1, $l^{\xi}=-1$, $|0\rangle\rightarrow|1\rangle$), TC conversion (AGM2, $l^{\xi}=2$, $|1\rangle\rightarrow|-1\rangle$) and conversion back into a plane wave (AGM3, $l^{\xi}=-1$, $|-1\rangle\rightarrow|0\rangle$), see figure 2(c). The geometric phase retrieved from the simulation is proportional to $\exp(2i\theta_l)$ where θ_l is the orientation of the 2nd AGM, as shown in figure 2(e). Similar to the spin-dependent optical geometric phase, the acoustic geometric phase also depends on the sign of TC of the input vortex. For example, when we invert the sign of TC of AGM1 from 1 to−1, the TC conversion process enabled by AGM2 becomes$|-1\rangle\rightarrow|1\rangle$, and the corresponding geometric phase is $\exp(-2i\theta_l)$. Moreover, the geometric-phase modulation obtained through higher order TC conversions, such as $|2\rangle\rightarrow|-1\rangle$ ($\propto\exp(3i\theta_l)$) and $|3\rangle\rightarrow|-1\rangle$ ($\propto\exp(4i\theta_l)$), are shown in supplementary material [36].

To showcase the potential of acoustic geometric phase in wavefront manipulation, we theoretically study the beam steering and beam focusing by using the ideal geometric-phase meta-arrays described above. Figure 3(a) shows the full-wave simulation of the beam steering via $|1\rangle\rightarrow|0\rangle$ TC conversion process. Similar to the meta-array pixel given in figure 2(b), two AGMs are utilized here to generate the input vortex (AGM1, $l^{\xi}=-1$, $|0\rangle\rightarrow|1\rangle$) and to encode the geometric phase (AGM2, $l^{\xi}=+1$, $|1\rangle\rightarrow|0\rangle$). In our study, the geometric-phase meta-array consists of 12 pixels, the operating wavelength λ_0 is selected as 12 cm, the pixel size p_{meta} is 9 cm, which is slightly larger than the outer diameter of waveguide (8 cm). The orientation angle θ_l of AGM2 is varied linearly along x direction, with a uniform step of 30°. The anomalous refracted angle retrieved from the calculated far-field is $-6.3°\pm0.1°$, which agrees well with the theoretical value obtained based on the geometric phase of θ_l. For the $|1\rangle\rightarrow|-1\rangle$ TC conversion process, the designed meta-array pixel consists of three AGMs as shown in figure 2(c), i.e. input vortex generation (AGM1, $l^{\xi}=-1$, $|0\rangle\rightarrow|1\rangle$), vortex conversion for geometric-phase modulation (AGM2, $l^{\xi}=+2$, $|1\rangle\rightarrow|-1\rangle$) and vortex detection for field reconstruction (AGM3, $l^{\xi}=-1$, $|-1\rangle\rightarrow|0\rangle$). The anomalous refracted angle obtained from the simulation is $-12.8°\pm0.1°$ (figure 3(b)), which agrees well with the theoretical value

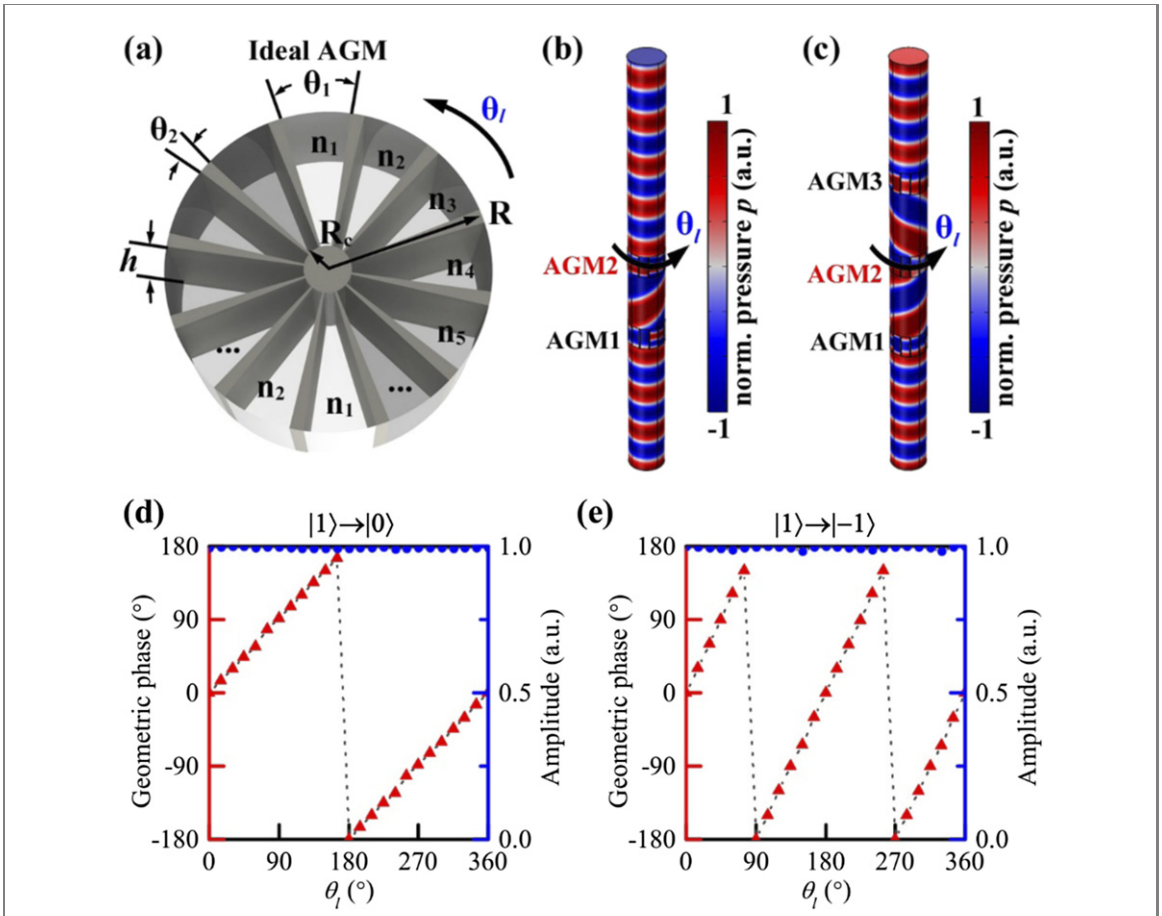

Figure 2. Geometric-phase modulation defined by TC conversion in acoustic meta-plates. Schematic of (a) ideal acoustic meta-plate, the radius of waveguide R and solid center R_c is $0.4\lambda_0$ and $0.05\lambda_0$, the thickness h of AGM is $0.5\lambda_0$, the section angle θ_1 and θ_2 is 27° and 3°, respectively. Configuration of the cascaded acoustic meta-plates for geometric phase encoding process (b) $|0\rangle \rightarrow |1\rangle \rightarrow |0\rangle$ and (c) $|0\rangle \rightarrow |1\rangle \rightarrow |-1\rangle \rightarrow |0\rangle$, and the corresponding geometric phase (red solid triangle) and transmitted amplitude (blue solid circle) obtained via TC conversion processes vs the orientation angle of AGM2 for (d) $|1\rangle \rightarrow |0\rangle$ and (e) $|1\rangle \rightarrow |-1\rangle$.

calculated according to the geometric phase of $2\theta_l$. Interestingly, by inverting the TC of AGM1 and AGM3 from $l^{\xi} = 1$ to $l^{\xi} = -1$, the geometric phase inverts its sign. Based on the geometric-phase pixel used in figure 3(a), we further show beam focusing realized by an acoustic geometric-phase metalens via $|1\rangle \rightarrow |0\rangle$ process, as shown by the left panel of figure 3(c). The phase profile for focusing in the x–z plane is $\varphi(x) = -k\left(f_z - \sqrt{x^2 + f_z^2}\right)$, where $k = 2\pi/\lambda_0$ is the operating wavenumber, the designed focal length f_z is $10\lambda_0$ and the orientation angle of AGM2 in each pixel follows exactly $\varphi(x)$. The top- and bottom-right panel of figure 3(c) show the field intensity profile along two perpendicular lines A and B across the focal point. The simulated focal length is about 1.16 m which is close to the designed value 1.2 m. Besides the focusing of free-space plane acoustic waves, other beam manipulations can also be readily achieved.

4. Discussion

Considering the realization of acoustic geometric-phase meta-array in real applications, we utilize realistic acoustic meta-structures to achieve wave manipulation based on the acoustic geometric phase. Here, the acoustic meta-atoms designed for different sections are classical Helmholtz resonator-straight pipe hybrid structures [37], as shown in figure 4(a). By tuning the widths of the open pipe (u_a, u_b, u_c) and the open neck (v_a, v_b, v_c) of the Helmholtz resonators of each layer, a high transmission can be achieved. Figure 4(a) shows the design of two meta-plates of TC $l^{\xi} = 1$ and $l^{\xi} = 2$, with the detailed geometry parameters of the constituent units given in supplementary material [36]. Here, AGMs of TC $l^{\xi} = 1$ and $l^{\xi} = 2$ are numerically investigated, and the optimized working frequency in our design is 2.88 kHz. Figure 4(b) shows the TC generation, conversion and detection with the above two types of AGMs, where the acoustic vortex sources are obtained by illuminating plane acoustic waves onto the meta-plate of TC $l^{\xi} = 1$. Figures 4(c) and (d) show the acoustic geometric phase (red solid triangle) and the corresponding transmitted

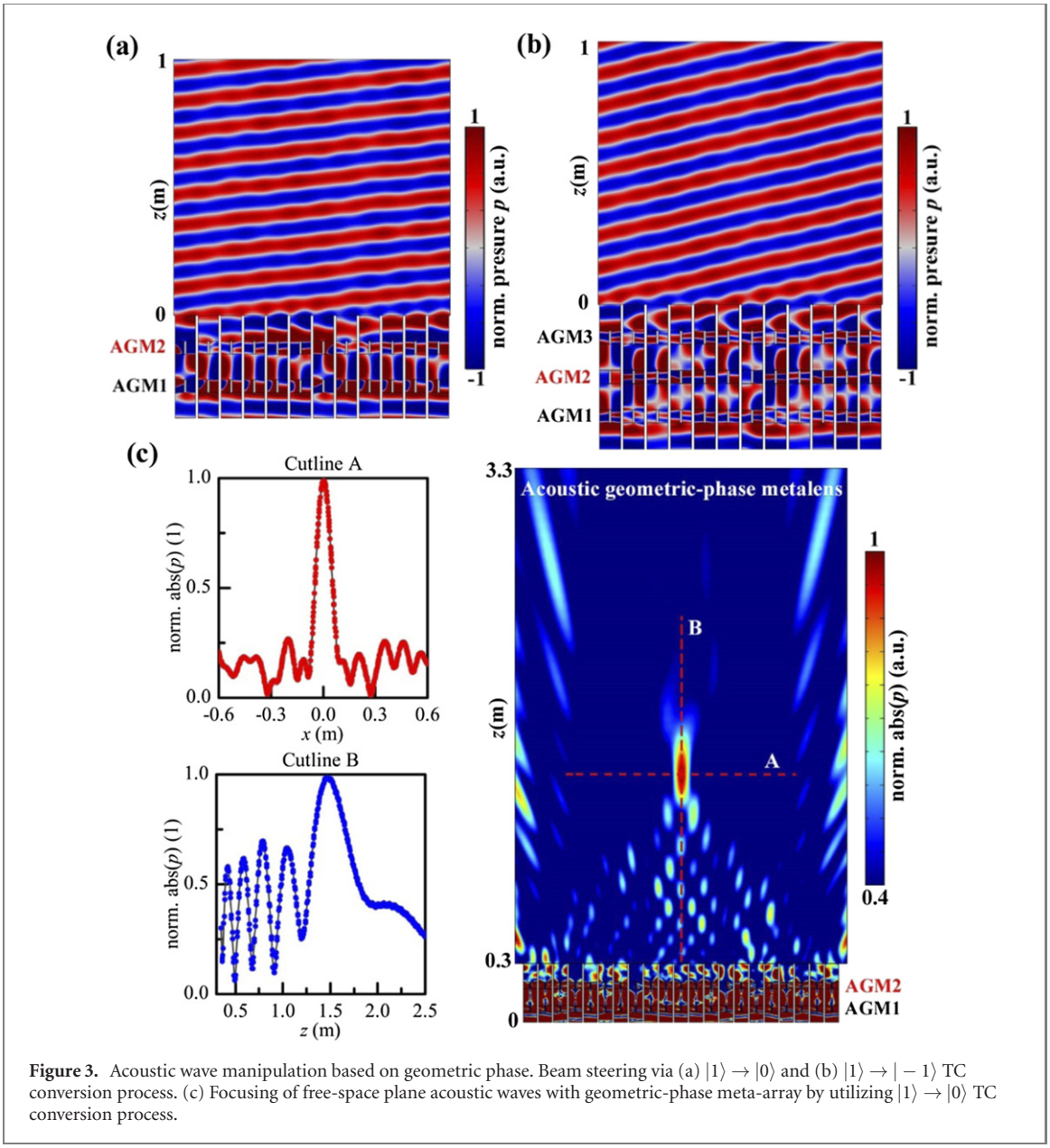

Figure 3. Acoustic wave manipulation based on geometric phase. Beam steering via (a) $|1\rangle \rightarrow |0\rangle$ and (b) $|1\rangle \rightarrow |-1\rangle$ TC conversion process. (c) Focusing of free-space plane acoustic waves with geometric-phase meta-array by utilizing $|1\rangle \rightarrow |0\rangle$ TC conversion process.

amplitude (blue solid circle) for two systems with cascaded AGMs for realizing geometric phase based on $|1\rangle \rightarrow |0\rangle$ and $|1\rangle \rightarrow |-1\rangle$ TC conversion processes, respectively. It is obvious that the geometric-phase modulation obtained with the realistic acoustic meta-plates agrees well with theoretical predictions. However, due to the multiple scattering induced by the realistic AGMs, the transmitted field uniformity and transmission efficiency would be deteriorated when more AGMs are cascaded. In our simulation, the distance between two meta-plates in $|1\rangle \rightarrow |0\rangle$ process shown in figure 4(c) and the interval among three meta-plates in $|1\rangle \rightarrow |-1\rangle$ process shown in figure 4(d) are optimized as 30 cm and 10 cm, respectively. It should be noted that the influence of thermal viscosity on the acoustic geometric-phase modulation is negligible (see supplementary material [36]). In supplementary material [36], we provide the full-wave simulation of broadband beam bending (from 1.9 kHz to 3.1 kHz) realized by a geometric-phase meta-array made up of the realistic acoustic meta-plates. It is found that our geometric-phase acoustic meta-array could operate in a broadband frequency range, benefitting from the dispersionless character of geometric phase.

In this work, the overall size of our acoustic geometric-phase meta-array mainly depends on the TC conversion process we utilize for the geometric-phase modulation. For higher order acoustic geometric phase, acoustic vortex of larger TC value requires bigger waveguide radius due to the consideration of the cutoff frequency. Therefore, here we only demonstrate the acoustic geometric-phase modulation obtained via $|1\rangle \rightarrow |0\rangle$ and $|1\rangle \rightarrow |-1\rangle$ processes, in which the radius of the waveguide is subwavelength. Another key factor that influences the thickness of the meta-array is the design strategy of AGM, where the

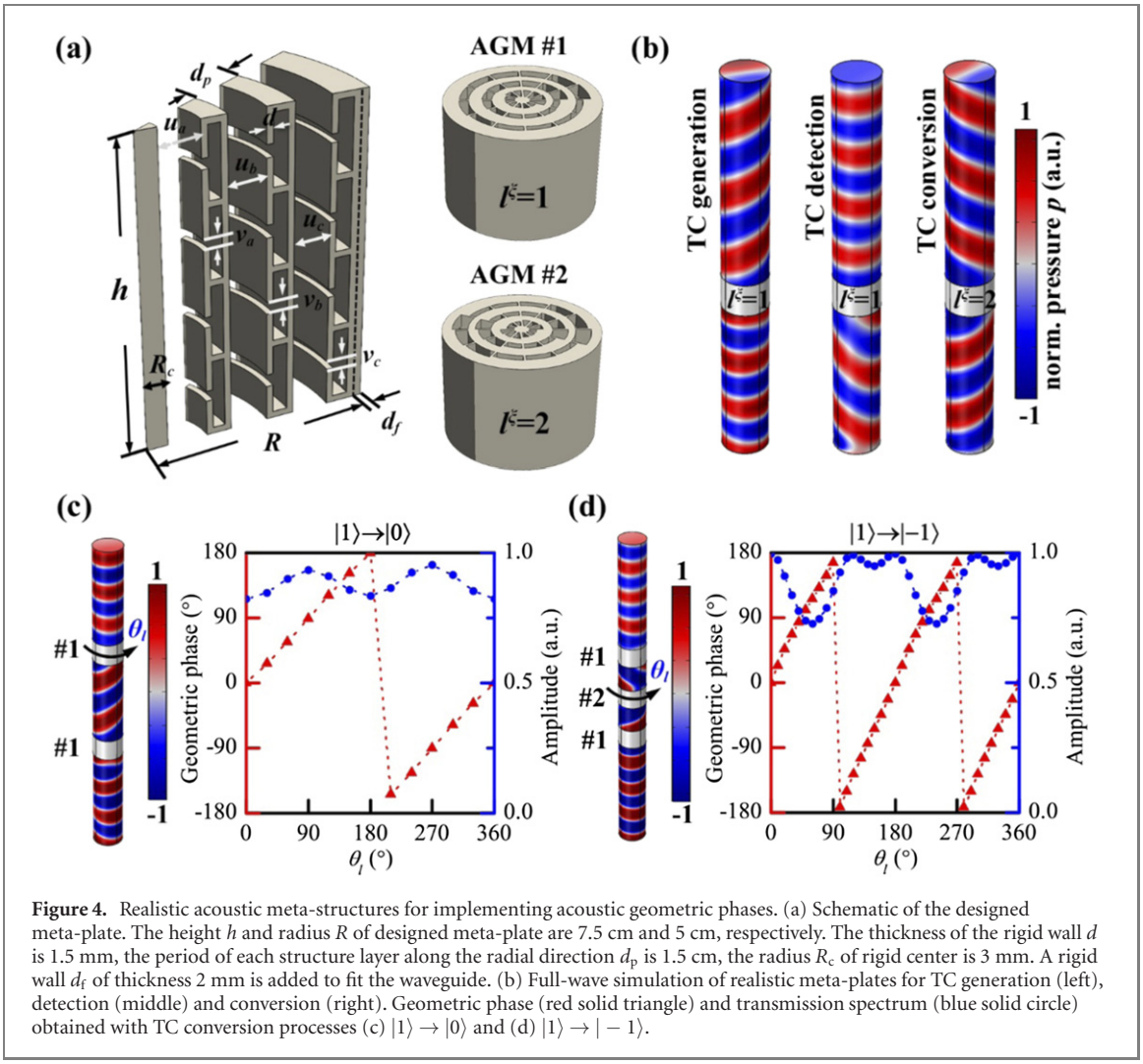

Figure 4. Realistic acoustic meta-structures for implementing acoustic geometric phases. (a) Schematic of the designed meta-plate. The height h and radius R of designed meta-plate are 7.5 cm and 5 cm, respectively. The thickness of the rigid wall d is 1.5 mm, the period of each structure layer along the radial direction d_p is 1.5 cm, the radius R_c of rigid center is 3 mm. A rigid wall d_f of thickness 2 mm is added to fit the waveguide. (b) Full-wave simulation of realistic meta-plates for TC generation (left), detection (middle) and conversion (right). Geometric phase (red solid triangle) and transmission spectrum (blue solid circle) obtained with TC conversion processes (c) $|1\rangle \rightarrow |0\rangle$ and (d) $|1\rangle \rightarrow |-1\rangle$.

AGM of smaller height is desired for the implementation of a more compact acoustic geometric-phase meta-array.

5. Conclusion

In summary, we have proposed the concept of acoustic geometric phase generated in the process of TC conversions, which is a generalization of optical geometric phase for spin conversion. Different from the conventional resonance-type phase modulation, which relies on the geometry and usually tangled with transmission amplitude, acoustic geometric phase is highly robust, and it enables arbitrary phase manipulation by simply rotating the meta-plates. Our work transfers the concept of optical geometric phase to acoustics, and shows its potential in constructing broadband and reconfigurable acoustic meta-devices for arbitrary field generations and manipulations.

Acknowledgments

The authors would like to thank Dr Junfei Li from Duke University for the fruitful discussions. We also thank Dr Yuhong Na (L) for the help in artistic figure rendering. This research was supported by National Nature Science Foundation of China (Grant Nos. 92050117, 61861136010, 12104044), Beijing Outstanding Young Scientist Program (Grant No. BJJWZYJH0120190007022), China Postdoctoral Science Foundation (Grant No. 2021M690410), the Research Grants Council of Hong Kong (AoE/P-502/20), and Sino-German (CSC-DAAD) Postdoc Scholarship Program, 2020 (Grant No. 57531629).

Data availability statement

All data that support the findings of this study are included within the article and supplementary file.

ORCID iDs

Lingling Huang https://orcid.org/0000-0002-3647-2128

References

[1] Hasman E, Kleiner V, Biener G and Niv A 2003 *Appl. Phys. Lett.* **82** 328
[2] Lin D, Fan P, Hasman E and Brongersma M L 2014 *Science* **345** 298
[3] Xiao S, Wang J, Liu F, Zhang S, Yin X and Li J 2017 *Nanophotonics* **6** 215–34
[4] Khorasaninejad M, Chen W T, Devlin R C, Oh J, Zhu A Y and Capasso F 2016 *Science* **352** 6290
[5] Wang S *et al* 2018 2018 *Nat. Nanotechnol.* **13** 3
[6] Huang L *et al* 2013 *Nat. Commun.* **4** 2808
[7] Zheng G, Mühlenbernd H, Kenney M, Li G, Zentgraf T and Zhang S 2015 *Nat. Nanotechnol.* **10** 308–12
[8] Chen S, Li G, Zeuner F, Wong W H, Pun E Y B, Zentgraf T, Cheah K W and Zhang S 2014 *Phys. Rev. Lett.* **113** 033901
[9] Tymchenko M, Gomez-Diaz J S, Lee J, Nookala N, Belkin M A and Alù A 2015 *Phys. Rev. Lett.* **115** 207403
[10] Chantakit T, Schlickriede C, Sain B, Meyer F, Weiss T, Chattham N and Zentgraf T 2020 *Photon. Res.* **8** 1435
[11] Zhu L *et al* 2020 *Sci. Adv.* **6** eabb6667
[12] Wang K *et al* 2018 *Science* **361** 1104
[13] Georgi P *et al* 2019 *Light Sci. Appl.* **8** 70
[14] Shi C, Zhao R, Long Y, Yang S, Wang Y, Chen H, Ren J and Zhang X 2019 *Natl. Sci. Rev.* **6** 707–12
[15] Blikoh K Y and Nori F 2019 *Phys. Rev.* B **99** 174310
[16] Zhang S, Yin L and Fang N 2009 *Phys. Rev. Lett.* **102** 194301
[17] Zhu Y, Fan X, Liang B, Cheng J and Jing Y 2017 *Phys. Rev.* X **7** 021034
[18] Li Y, Qi S and Assouar M B 2016 *New J. Phys.* **18** 043024
[19] Fu Y, Shen C, Zhu X, Li J, Liu Y, Cummer S A and Xu Y 2020 *Sci. Adv.* **6** eaba9876
[20] Jiang X, Liang B, Cheng J-C and Qiu C-W 2018 *Adv. Mater.* **30** 1800257
[21] Zhao J, Li B, Chen Z N and Qiu C-W 2013 *Appl. Phys. Lett.* **103** 151604
[22] Wu X, Xia X, Tian J, Liu Z and Wen W 2016 *Appl. Phys. Lett.* **108** 163502
[23] Díaz-Rubio A, Li J, Shen C, Cummer S A and Tretyakov S A 2019 *Sci. Adv.* **5** eaau7288
[24] Hou Z, Ding H, Wang N, Fang X and Li Y 2021 *Phys. Rev. Appl.* **16** 014002
[25] Liang Z and Li J 2012 *Phys. Rev. Lett.* **108** 114301
[26] Li Y, Liang B, Tao X, Zhu X-f, Zou X-y and Cheng J-c 2012 *Appl. Phys. Lett.* **101** 233508
[27] Xie Y, Wang W, Chen H, Konneker A, Popa B-I and Cummer S A 2014 *Nat. Commun.* **5** 5553
[28] Zhu X, Li K, Zhang P, Zhu J, Zhang J, Tian C and Liu S 2016 *Nat. Commun.* **7** 11731
[29] Esfahlani H, Lissek H and Mosig J R 2017 *Phys. Rev.* B **95** 024312
[30] Tian Y, Wei Q, Cheng Y, Xu Z and Liu X 2015 *Appl. Phys. Lett.* **107** 221906
[31] Ma G, Yang M, Xiao S, Yang Z and Sheng P 2014 *Nat. Mater.* **13** 873–8
[32] Memoli G, Caleap M, Asakawa M, Sahoo D R, Drinkwater B W and Subramanian S 2017 *Nat. Commun.* **8** 14608
[33] Zhao S, Chen A, Wang Y and Zhang C 2018 *Phys. Rev. Appl.* **10** 054066
[34] Tian Z, Shen C, Li J, Reit E, Gu Y, Fu H, Cummer S A and Huang T J 2019 *Adv. Funct. Mater.* **29** 13
[35] Zhang C, Cao W K, Wu L T, Ke J C, Jing Y, Cui T J and Cheng Q 2021 *Appl. Phys. Lett.* **118** 133502
[36] See supplementary material for additional discussions on the geometric-phase obtained by rotating the acoustic vortex sources, acoustic geometric-phase modulation obtained with phased microphone illumination, geometry parameters of meta-plate and the influence of thermal viscosity on the performance of designed geometric-phase meta-plate, broadband acoustic beam bending realized with real geometric-phase meta-array, detailed setup of the FEM simulation.
[37] Jiang X, Li Y, Liang B, Cheng J C and Zhang L 2016 *Phys. Rev. Lett.* **117** 034301